First order optical interference between distinguishable photon paths.

M. Fernández-Guasti[1]

[1]Lab. de Óptica Cuántica, Depto. de Física, Universidad Autónoma Metropolitana, - Iztapalapa, C.P. 09340 Ciudad de México, Ap. postal. 55-534, MEXICO
e-mail: mfg@xanum.uam.mx, url: https://luz.izt.uam.mx

Abstract—A necessary condition in order to obtain interference fringes in QED is the existence of at least two possible paths and unknown which-path information. If the photon beams have different frequencies, stability of the sources and fast enough detectors are also required. In this experiment, first order interference between two truly independent CW Nd:YAG monomode laser sources was produced. Contrary to what is expected, interference is observed although the photon beams are distinguishable and the path is unequivocally known for each photon beam. Segments of the ultra-stabilized CW wavetrains are selected with an acousto optic modulator. Temporal and spatial interference are integrated in a single combined phenomenon via streak camera detection. In this way, interference fringes and frequency beating are both present in the streak camera images. The photon beams are labeled with two slightly different frequencies. In addition, the inclination of the beams establish the projection of their respective wave vectors in the detection plane, which may be seen as perturbations coming from two different slits. The fringes displacement in the time-space interferograms reveal the trajectories of the frequency labeled photons. Since the detection probability of any one photon is independent from the detection of the rest, the trajectory can be drawn for each frequency labeled event. These results indicate that in non-degenerate frequency schemes, the ontology has to be refined and the which path criterion must be precisely stated. If reference is made to the frequency labeled photons, the path of each photon is known, whereas if the query is stated in terms of the detected photons, the path is unknown.

1. INTRODUCTION

Interference of waves can take place in the spatial or the temporal domain. The former produces i) spatial interference fringes and the latter ii) temporal interference or beating. The beams in optical spatial interference setups are usually derived from the same source but traveling along separate paths. In contrast, temporal interference is commonly achieved with different sources having different frequencies. For a constant frequency difference, a single laser source is commonly used. The frequency of one beam can then be shifted with an acousto optic modulator [1] or by selecting different frequencies from a spatially chirped femtosecond pulsed source [2]. If separate lasers are used, the frequency difference varies from shot to shot and so does the fringe pattern [3].

First order interference involves correlations between the fields whereas second order interference involves correlations between the fields' intensities. These correlations can be described with semi-classical (continuum) field theory (CFT) or quantum field theory (QFT). The archetypal Young's two slit interference experiment exhibits the same first order interference patterns when produced by short exposure intense light sources or by long exposure accumulation with feeble light. However, the ontology in the two theories is quite different. CFT invokes a well defined amplitude and phase correlation between the two interfering fields during the detector integration time [4]. In QFT, interference takes place only when the path of the photons is unknown [5].

The standard formulation of the quantum which path problem is that a measurement which shows which slit the photon passed through perturbs the system to such an extent that no interference fringes are detected [6, p.22]. We show here that interference with which-path certainty is possible if the statement is made with respect to the photon label (red or blue in these experiments) but without reference to a detected photon. Our observations are consistent with Heisenberg's uncertainty principle but compromise some versions of Bohr's complementary principle.

2. EXPERIMENTAL CONSIDERATIONS AND SETUP

Photons were generated from two independent Nd:YAG lasers codenamed *cheb* and *oxeb* [1]. These continuous wave (CW), monomode lasers (AOTK 532Q) have a coherence time greater than 300 ns [7]. The operation of each laser does not rely in any way on the working of the other laser, nor are they synchronized. The wavelengths of the two lasers, measured with an spectrometer (Spex1704 with 0.01 nm resolution), were temperature tuned so that their frequencies were sufficiently close to be resolved by a streak camera (Optronis SC-10). The two laser beams were steered with mirrors into a TeO_2 acousto optic modulator (AOM) (10/10 ns, 10 to 90% rise/fall time for a 55 μm beam-waist). Delay generator pulses with 700 ns width produced temporal slices of the CW beam. The general setup is shown in figure 1. A two slit wavefront division interferometer is emulated throughout the trajectories. The expanded collimated beams were overlapped and detected with the streak camera. In the streak camera, also called optical oscilloscope, light impinges on a photocathode placed on the inner part of a vacuum tube. The electrons emitted by the photocathode (8 mm x 2 mm) are accelerated and swept in the perpendicular direction to its long axis, so that a two dimensional image is produced. Each photoelectron thereafter impacts on a multichannel plate (MCP) and is cascaded so that the bunch of electrons produces a spot as it reaches a phosphor screen. The MCP amplification voltage is adjusted so that the intensity of this spot is adequately detected by a CCD camera. At low intensity levels, the device can be operated in photon counting mode. In the streak camera plots, the abscissa represents time whereas the ordinate represents a transverse spatial coordinate. The density of white spots is proportional to the photon density in the two dimensional time-space coordinates. Streak images cannot be accumulated in this setup because the frequency and relative phase between the two lasers vary stochastically in time at scales larger than the coherence time. Therefore, the fringe pattern was recorded in single exposures with time durations of the order of the coherence time. Low repetition rates between 1 and 3 Hz were used to acquire images in real time. In the transverse dimensions, the x direction is limited to $x = 0 \pm 7.5\,\mu$m by a $\delta x = 15\,\mu$m entrance slit; In the y direction, the position detection range is 15 mm with $\delta y = 70\,\mu$m resolution. The temporal sweep is performed in the x direction with 0.34 % resolution of the full sweep time. This instrumental integration together with the image amplification and digitalization establishes the resolution of the apparatus. The low noise photocathode has a 10.37 % quantum efficiency (QE) at 532 nm and a dark noise of $100\,e^-/\text{cm}^2\text{s}$ (Photek ST-LNS20).

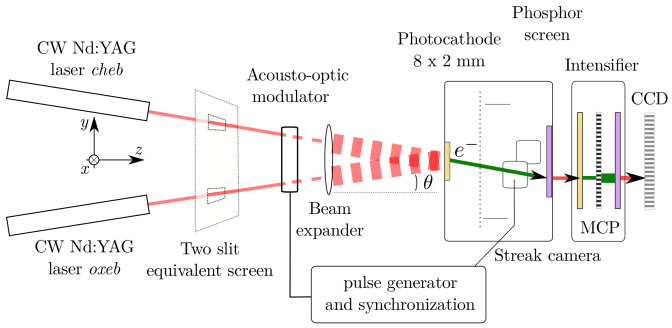

Figure 1: Schematic diagram of the experimental arrangement. The setup is equivalent to a Young's two slit experiment but each 'slit' is illuminated by an independent laser. The slits can be conceived to be placed at any plane between the sources and the photocathode detector before the beams overlap.

In a conventional single source Young's experiment, the slits separate the wavefront into two distinct wavefronts. Here, the wavefronts emanate from two different sources. The physical setup can be conceived as each of the sources illuminating a slit. The plane where the slits are placed is any plane between the sources and the plane where the beams begin to overlap just before the interfering detection plane. Furthermore, each slit could be placed at a different plane, reminiscent of second order interference patterns produced by non-local objects [8].

2.1. Photon labeling

The two collimated beams are incident on the streak camera photocathode with a 0.14 mrad angle between them in order to have comfortably resolved fringe maxima separated by 1.88 mm. Cartesian coordinates are set with z normal to the detector surface and the fields are linearly polarized in

[1] Tseltal variant of Mayan language for numbers two → *cheb* and three → *oxeb*.

the x direction. The two wave-fields propagate in the (y,z) plane, paraxially to the z direction at a small but opposite angle θ in the y axis. The wave vector of the field coming from the cheb laser is

$$\mathbf{k}_1 = \mathbf{k}_{y1} + \mathbf{k}_{z1} = -k_1 \sin\theta\, \hat{\mathbf{e}}_y + k_1 \cos\theta\, \hat{\mathbf{e}}_z,$$

and the wavefield coming from the oxeb laser is

$$\mathbf{k}_2 = \mathbf{k}_{y2} + \mathbf{k}_{z2} = k_2 \sin\theta\, \hat{\mathbf{e}}_y + k_2 \cos\theta\, \hat{\mathbf{e}}_z,$$

where $|\mathbf{k}_1| = k_1 = \frac{\omega_1}{c}$ and $|\mathbf{k}_2| = k_2 = \frac{\omega_2}{c}$ are the respective wave vector magnitudes and $\hat{\mathbf{e}}_y, \hat{\mathbf{e}}_z$ are unit vectors in the y and z directions. The y axis positive direction has been set in the same direction of $\mathbf{k}_{y2}$, that is, the photons coming from the oxeb laser have positive momentum, $\hbar\mathbf{k}_{y2} = \hbar\,|\mathbf{k}_{y2}|\,\hat{\mathbf{e}}_y$ in the y direction at the detector plane. In addition, the photons are also labeled by their frequency. Since each laser source has its specific frequency, the wavefield from the *oxeb* laser with momentum projection $\hbar\mathbf{k}_{y2}$ has frequency ω_2 and the wavefield from the *cheb* laser with momentum projection $\hbar\mathbf{k}_{y1}$ has frequency ω_1. The wave vector projection in the transverse y direction and the corresponding frequency are highly correlated. This so-called labeling of the photons is similar to the temporal and spatial labeling terminology in HOM second order interferometers [9].

2.2. QFT description

In QFT, the two quantized complex electric field operators with linear polarization are $\hat{E}_1^{(+)}(\mathbf{r}) = i\mathcal{E}_1^{(1)} \exp(i\,\mathbf{k}_1 \cdot \mathbf{r})\,\hat{a}_1$ and $\hat{E}_2^{(+)}(\mathbf{r}) = i\mathcal{E}_2^{(1)} \exp(i\,\mathbf{k}_2 \cdot \mathbf{r})\,\hat{a}_2$, where $\mathcal{E}_1^{(1)}$, $\mathcal{E}_2^{(1)}$ are the one-photon amplitudes and $\hat{a}_1$, $\hat{a}_2$ are the annihilation operators for modes 1 and 2 respectively. The fields from each monomode laser are adequately represented by single mode coherent states $|\alpha_1\rangle$ and $|\alpha_2\rangle$ [10]. Since the two fields are independent, their superposition is a two mode factorizable state, $|\psi_{1,2-qc}(t)\rangle = |\alpha_1 \exp(-i\omega_1 t)\rangle\,|\alpha_2 \exp(-i\omega_2 t)\rangle$. These states allow for the factorization of the first order coherence function [11]. The quantum photo detection probability is

$$w(\mathbf{r},t) = s\left(\mathcal{E}_1^{(1)}\mathcal{E}_2^{(1)}\right)^2 \left(|\alpha_1|^2 + |\alpha_2|^2 + \alpha_1^*\alpha_2 \exp\left[i\left((\mathbf{k}_2 - \mathbf{k}_1)\cdot\mathbf{r} - \triangle\omega\, t + \triangle\varphi\right)\right] + c.c.\right), \quad (1)$$

where s is the sensitivity of the detector, $\triangle\omega = \omega_2 - \omega_1$ and $\triangle\varphi = \varphi_2 - \varphi_1$ is the phase difference due to the independent stochastic functions with coherence times τ_1, τ_2 due to the laser cavities' instabilities.

The spatially dependent interference argument is $(\mathbf{k}_2 - \mathbf{k}_1)\cdot\mathbf{r} = 2\bar{k}\sin\theta\; y + \triangle k \cos\theta\; z$, where $2\bar{k} = k_1 + k_2$, $\triangle k = k_2 - k_1$. The field is observed at a detector placed at the $z = z_0$ plane, thus the term $\triangle k \cos\theta\, z_0$, only adds a constant phase shift. The phase as a function of time and the transverse distance y is

$$\phi = 2\bar{k}\sin\theta\; y + \triangle k\cos\theta\, z_0 - \triangle\omega\, t + \triangle\varphi, \quad (2)$$

When two different frequencies are present, the equiphase surfaces evolve in time and space. In contrast, wave-fronts in frequency degenerate setups entail spatial coordinates alone. The velocity of an equiphase plane, provided that $\triangle\varphi$ does not vary appreciable during the measurement, is

$$\frac{dy}{dt} = \frac{\triangle\omega}{2\bar{k}\sin\theta}. \quad (3)$$

The fringes are thus displaced in time with a slope $\frac{dy}{dt}$, whose sign is determined by the value of $\triangle\omega$, the frequency difference between the two sources.

3. RESULTS

Each point in the streak camera image represents a quantum test of whether a photon arrived at position y of the streak camera photocathode where the two photon beams overlap, at a given time t. A streak camera image consists of two sets of quantum tests, one in the spatial domain and another in the temporal domain. In the y ordinate direction, electrons in the photocathode long axis act as a set of spatially distributed detectors. For each y position, there is another set of different consecutive quantum tests that probe the dynamical evolution of the quantum system [12, p.33, p.237]. This set is depicted in the abscissas time axis. A photoelectron is emitted at the

streak camera photocathode with 10.37% quantum efficiency if a photon is present at (y,t) where the photon beams overlap. These events are amplified by the MCP and discretized in the $1024 \times 1392 = 1.425 \times 10^6$ detectors at the CCD. Thus, each streak camera interferogram involves about 10^6 quantum tests. The interferograms in figures 2 and 3 were registered at 50 ns/mm sweep speed with 3.4 ns temporal resolution. The transverse spatial range is 15 mm with 70 μ resolution. The 655 ns segments obtained with the AOM modulator, where the two CW lasers temporally overlap, exhibit high contrast interference fringes with visibility above 70%.

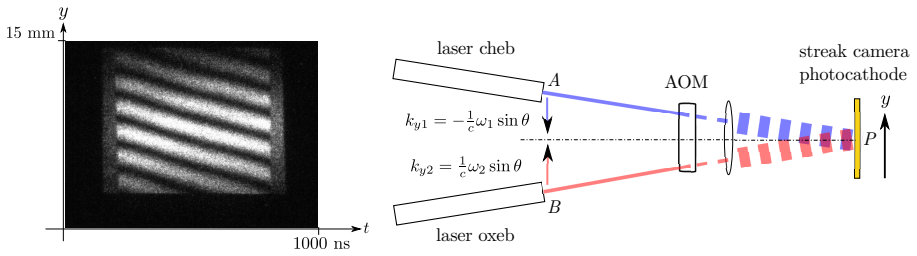

Figure 2: The steak camera image (left) shows negative slope interference fringes. Therefore, the oxeb laser emitted lower frequency photons that followed the path $\overline{BP}$. The higher frequency photons from the cheb laser followed the path $\overline{AP}$.

The slope of the fringes in the interferogram shown in figure 2 is negative. From Eq. (3), if the slope of the equiphase lines is negative, the frequency difference $\triangle\omega$ is negative and thus $\omega_2 < \omega_1$. Therefore, the oxeb laser emitted photons with lower energy $\hbar\omega_2$, drawn in red in figure 2. These photons, with positive linear momentum projection $\hbar\mathbf{k}_{y2}$ in the y direction, ineluctably followed the path $\overline{BP}$, where B is the position of the beam at the laser oxeb output and P is a point in the streak camera photocathode screen. The converse is true for the photons that comprise the cheb laser beam. These higher energy photons drawn in blue in figure 2, have negative linear momentum projection $-\hbar\,|\mathbf{k}_{y1}|\,\hat{\mathbf{e}}_y$ at the detector plane. They followed the path $\overline{AP}$, where A is the position of the beam at the cheb laser output. From the time-space interferogram, it is of course possible to evaluate the frequency difference $\triangle\omega = -19.4$ MHz, although the specific value is irrelevant for the argumentation.

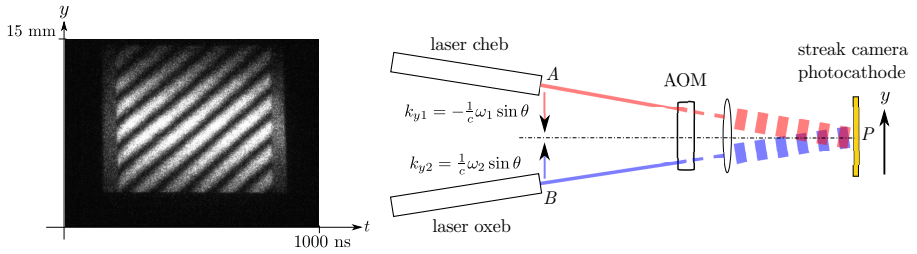

Figure 3: Positive slope interference fringes, the oxeb laser emitted higher frequency photons than the cheb laser. Photons from the oxeb laser followed the lower path $\overline{BP}$ whereas photons from the cheb laser followed the upper path $\overline{AP}$.

The interferogram shown in figure 3, was acquired 1014 ms after the interferogram shown in figure 2. The lasers' frequency drifted so that the slope changed sign from one scan to the next. For a positive slope, the frequency difference $\triangle\omega$ is positive and thus $\omega_2 > \omega_1$. Therefore, the oxeb laser emitted photons with higher energy $\hbar\omega_2$, drawn in blue in figure 3. These higher energy photons again necessarily followed the path $\overline{BP}$. The photons emitted by the cheb laser beam now have lower energy and followed the path $\overline{AP}$. In this case, $\triangle\omega = 54.9$ MHz. Summing up the two previous results: *The fringes are displaced, as a function of time, in the same direction of the transverse momentum projection of the photons with higher energy.*

If for some odd reason, in the exposure of figure 3, some red photons had positive momentum (came from the lower slit) and some blue ones had negative momentum (came from the upper slit), they would produce a negative slope. However, the interferogram in figure 3 does not exhibit even the faintest fringes with negative slope, thus this possibility is ruled out. Thus, in this case, the blue photons necessarily followed the path $\overline{BP}$ and the red photons followed the path $\overline{AP}$. Therefore,

we must conclude that in either case ($\omega_2 \lessgtr \omega_1$), the trajectory of the photons is well defined, yet a high contrast interference pattern is observed.

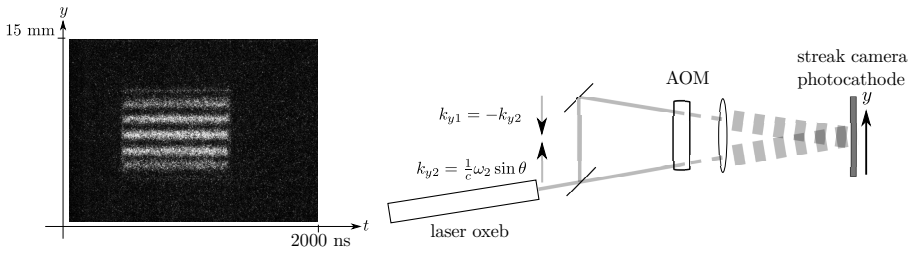

Figure 4: Zero slope interference fringes. Photons are no longer frequency distinguished.

Consider for completeness, the case where the frequencies are equal. This condition is easier to achieve experimentally using the same laser source but it could actually be accomplished with two laser sources with the appropriate stability and bandwidth. In this case, interference fringes have zero slope and the pattern is constant in time as shown in figure 4. There is no frequency labeling of the photons and it is not possible to deduce which path they followed. There is still a momentum labeling but, due to the position-momentum uncertainty, the sources are unresolved at the detector [13].

4. EVALUATION OF QUANTUM UNCERTAINTIES

In order to establish the photons path, it is sufficient to measure whether the fringes displacement is positive or negative. Nonetheless, it is reassuring to confirm that the actual numerical values of the measurements do not violate an uncertainty relationship, nor are they buried below the quantum noise. For a 10 mW average power with angular frequency $\omega_\ell = 3.54 \times 10^{15}$ Hz, the average number of photons per nanosecond is $\Phi^{\rm ph} = \frac{\Phi}{\hbar\omega_\ell} = 2.68 \times 10^7$ photons $\cdot$ ns^{-1}. The $\delta x = 15\,\mu$ horizontal entrance slit reduces the power by a factor of 10^{-3} and the QE of the photodetector by 1.037×10^{-1}. The average number of photons detected per nanosecond is then $\Phi^{\rm ph} = 2.68 \times 10^3$ photons $\cdot$ ns^{-1}. The standard deviation in the number of photons is thus $\sqrt{\langle N_\ell\rangle} = \sqrt{\Phi^{\rm ph}} = \sqrt{2.68 \times 10^3} = 51.7$. The phase uncertainty in the standard quantum limit (SQL) [14] in one nanosecond is then approximately $\triangle\phi_{\rm SQL} = 1/2\sqrt{\langle N_\ell\rangle} = 9.66 \times 10^{-3} \approx 10^{-2}$ radians. This value of the SQL establishes the minimum achievable uncertainty in the phase of each photon beam at the detector. The spatial resolution between maxima located 1.88 mm apart, due to the sources' phase uncertainty $\triangle\phi_{\rm SQL}$ per nanosecond is $3\,\mu$m. The spatial frequency measurement uncertainty due to the interference of the two photon beams in our experiment is about 8 times larger than the SQL of each laser source.

The existence of an energy-time uncertainty relation has been subject to much debate [15, 16]. Due to the lack of a self-adjoint time operator, there is no quantum uncertainty relationship of time with any other dynamical variable [17], in particular energy or linear momentum. Nonetheless, time and frequency are, of course, Fourier transform conjugate variables subject to the inequality, $\delta t\,\delta\omega \geq \frac{1}{2}$ for Gaussian pulses based on the mean square deviation [18, p.623]. In quantum parlance, photons in different modes are distiguishable if the detection time is longer than the inverse of the modes frequency separation. Photons in modes separated by $\triangle\omega = 54.9$ MHz are distinguishable if they are detected in times longer than $1/\triangle\omega \approx 18$ ns. The detection in the present experiment is performed in successive time measurements over a time span larger than 603 ns.

In the limit of macroscopic fields and small quantum fluctuations, photon number N_ℓ and phase ϕ_ℓ fluctuations ($\ell = 1, 2$), look like complementary variables in the usual sense of quantum mechanics $\triangle N_\ell \triangle\phi_\ell \geq \frac{1}{2}$ [10, p. 368]. For minimum uncertainty states and in particular for coherent states, the equality is fulfilled (fluctuations are proportional to the square root of the average number of particles in a Poisson distribution)

$$\triangle\phi_\ell = \frac{1}{2\sqrt{\langle N_\ell\rangle}}.$$

The time-space interferograms shown here nicely depict the trend of this behaviour. For a few scattered dots, $\langle N_\ell\rangle$ is small and constant phase lines are difficult to establish. However, as the

number of dots increase, the equiphase lines become better delineated and their uncertainty is thus reduced. The number of detected events N_ℓ can be varied, either by attenuation of the sources or by evaluation of a limited portion of the interferogram. In the latter case, if the slope is evaluated from a partial region of the image, the number of dots is smaller and the uncertainty in the phase (slope) becomes larger.

5. DISCUSSION

Many which-path experiments have been tried out without success. So called welcher weg experiments were even proposed by eminent physicists, Einstein and Feynman amongst them [19, Sec.1.1.3]. The less disruptive probes implemented so far involve weak measurements that provide fuzzy quantum information [20, 21]. Our setup, designed to study the dynamics of decoherence, was not intended to undertake a which-path problem; The before mentioned facts being enough to deter almost anyone from doing so. Nonetheless, we should also mention that interference experiments with photons of different energy were already indicative of a well-known frequency going to a specific slit [22, 23].

Why then does this experiment succeed in the measurement of path knowledge without destroying the interference pattern? From our understanding, there are three reasons:

1. *The path information is obtained from measurements at the interference detection plane.* The trajectory is in no way perturbed since the path detection is not performed in mid trajectory but at the end plane where the fringes are observed. Recall that no information can be obtained without disturbance [24, P. Busch, Quantum Limitations of Measurement]. Furthermore, the Englert inequality establishes that for a given fringe visibility there is an upper bound on the amount of information that can be stored in a which-way detector (WWD) [25]. In the present experiment, photons are destroyed when detected at the streak camera photo-cathode where information is extracted, thus Busch theorem is not violated. Englert inequality is derived assuming that the WWD's are placed before the photon beams overlap. Here, the photocathode plays the role of the WWD's; However, it is placed at the interference plane where the beams overlap but not before.

2. *The fringes slope in the time-space coordinates is the decisive parameter in order to establish the photons path.*

   (a) A sufficiently large number of photons need to accumulate to produce a fringe pattern. Whether this pattern is obtained by intense or attenuated beam exposures does not alter the statistics of the laser light and are thus entirely equivalent [26]. It does not make sense to ask whether a single photon produces a fringe pattern. Nonetheless, the collection of measurements gives information about each trial even to the point of stating that "Each photon then interferes only with itself" [27, p.9]. In an analogous fashion, the trajectory of the photons is revealed here from the measurement of a large number of events. Nonetheless, information about the trajectory of each photon is obtained.

   (b) Successive time measurements of the fringe pattern are recorded. This scheme follows the rationale of quantum measurements distributed in time where the path-integral formulation is particularly well suited to describe the problem [28]. Feynman's rules for combining probability amplitudes depend on whether intermediate states are measured [29]. In the present experiment no intermediate state is measured. Nonetheless, information about intermediate states is obtained from measurements at a succession of final states.

3. *Photons need to be frequency labeled.* In general, photons need to be doubly labeled with tags that are not conjugate variables. In this experiment, labels are 'photon linear momentum projection in the y axis' and 'photon energy' or quantities derived thereof. Thus determination of one of them does not obstruct the determination of the other.

The notion of a photon arises naturally in number states as the elementary energy unit $\hbar\omega$. Number states are eigenstates of the Hamiltonian but their phase is random. In order to observe first order interference, a well defined phase, up to uncertainty limitations, is required. Single mode coherent states exhibit a well defined phase but are not eigenstates of the Hamiltonian. Their energy is not well defined due to the uncertainty in photon number but, being single mode states, the

energy per photon is fixed. In this experiment, the frequency label is essential but the number of photons is irrelevant as long as there are enough of them to establish fringes. Photons at the detection plane carry the phase information given by (2). They must have this information as revealed by the observed fringe pattern. If the position-momentum uncertainty or the energy uncertainty of coherent states were hindering the linear momentum projection or energy per photon, the interference pattern would be washed out contrary to what is observed.

The uncertainty principle has been stated as "Any determination of the alternative taken by a process capable of following more than one alternative destroys the interference between alternatives" [30, 1-2 The uncertainty principle, p.9]. This assertion is certainly compromised by the present results. However, Heisenberg's uncertainty principle is, strictly speaking, related to the uncertainty between conjugate variables, that is, operators that do not commute [12]. The present results do not contradict Heisenberg's uncertainty principle.

6. ONTOLOGY AND CONCLUSION

In the prevailing Copenhagen view of quantum mechanics, the theory is intrinsically probabilistic. A prediction can only be related to observation in an statistical way given by Born's rule. The larger the number of measured events, the sharper the measured property (within the uncertainty principle if complementary variables are involved). From the measurement of a large number of independent events, it is possible to infer certain properties of each event. The fundamental reason being that independence implies that each event is not altered in any way by the other events.

Let us pose two questions that are seemingly the same but have different answers:

- Do the experimental results reveal which path each photon followed?

The answer is YES. Let the outcome of the 10^6 quantum tests be positive slope fringes. Then, each red photon came through A and each blue photon came through B. The path that each photon followed is known, yet, an interference pattern is observed.

The interference pattern is built up by the superposition of red and blue photons. All the red photons came through slit A whereas all blue photons came through slit B. The certainty of the assertion depends on the visibility of the interference fringes, and these in turn, depend on the number of quantum events (and of course, the appropriate experimental arrangement with truly independent sources).

- Do the experimental results reveal which path did a detected photon (a white speck on the screen) followed?

The answer is NO. When we refer to 'this' photon that impinged on the screen, it is not known whether it is a red or a blue photon or even a redblue photon. In order to specify which way it followed, the colour must be known but we only detect a white speck regardless of the photon frequency. Thus interference is observed but the detected photon path is unknown.

The subtle but fundamental difference between these two queries is that the former question does not involve the category of the detected entity. In contrast, the detected entity is at the core of the latter question.

In order to reconcile both views, two alternatives are envisaged: *i) Detected photons are either blue or red.* One possibility would be to consider that a detected photon is either blue or red but its frequency cannot be known if interference occurs. An asset of this approach is that the entities 'red photon' or 'blue photon' retain their identity. Thus, the photon concept remains a good concept, in the sense of good quantum numbers. However, this view has the major problem that there is then no superposition of the disturbances, but it is superposition that produces the interference phenomenon. A thought experiment has been proposed before, involving frequency sensitive photo detectors with different predictions for the expected outcome [22, App. A]. It has also been stressed that superposition actually takes place only in the presence of charges that respond to the superimposed fields [31]. *ii) Detected photons bear information of both frequencies.* The other possibility to reconcile both views is to consider that a detected photon within the interference region has information on both laser fields as described by Paul [32, p.221]. In the present experiment, it must bear information of both frequencies according to the superposition described in subsection 2.2. The difficulty with this view is that a photon cannot give part of it to another photon because it would then loose its entity. Somehow, it has to give information to the other photon while retaining its photon identity. Recall that the photon concept is well defined in number

states but somewhat blurred in coherent states where the photon number is undefined. According with these two views, either the photon entity is well defined but the interference phenomenon is not neatly described, or the nature of the photon is blurred but the interference phenomenon is readily incorporated.

The which way assertion should then be refined in order to have an unambiguous meaning: The path that each photon followed can be known without destroying the interference pattern. In this formulation of the statement, the slit that each photon passed through is known, but it is not known to which detected photon it corresponds. Another, equally correct formulation is that, within the interference region, the path of a detected photon cannot be traced back. That is, if interference occurs, it is not possible to assert the path followed by a photon detected on the screen.

ACKNOWLEDGMENT

Part of the equipment used in these experiments was funded by CONACYT, projects CB2005-51345-F-24696 and CB2010-151137-F.

REFERENCES

1. L. M. Davis, "Interference between resolvable wavelengths with single-photon resolved detection," *Phys. Rev. Lett.*, vol. 60, p. 1258–1261, Mar 1988.
2. I. G. Saveliev, M. Sanz, and N. Garcia, "Time-resolved Young's interference and decoherence," *J. Opt. B*, vol. 4, p. S477–S481, 2002.
3. F. Louradour, F. Reyanud, E. Colombeau, and C. Froehly, "Interference fringes between two separate lasers," *Am. J. Phys.*, vol. 61, no. 3, p. 242–245, 1993.
4. A. S. Marathay, *Elements of Optical Coherence Theory*. 1982.
5. U. Eichmann, J. C. Bergquist, J. J. Bollinger, J. M. Gilligan, W. M. Itano, D. J. Wineland, and M. G. Raizen, "Young's interference experiment with light scattered from two atoms," *Phys. Rev. Lett.*, vol. 70, p. 2359–2362, Apr 1993.
6. G. Esposito, G. Marmo, G. Miele, and G. Sudarshan, *Advanced Concepts in Quantum Mechanics*. Cambridge: CUP, 2014.
7. M. Fernández-Guasti, H. Palafox, and R. Chandrasekar, "Coherence and frequency spectrum of a Nd:YAG laser - generation and observation devices," in *Optics and Photonics 2011*, vol. 8121 of *The nature of light: What are photons? IV*, p. 81211E–1–10, SPIE, 2011.
8. I. Vidal, D. P. Caetano, E. J. S. Fonseca, and J. M. Hickmann, "Observation of interference pattern in the intensity correlation of a non-local object using a Hanbury Brown and Twiss-type experiment," *EPL (Europhysics Letters)*, vol. 82, no. 3, p. 34004, 2008.
9. P. S. K. Lee and M. P. van Exter, "Spatial labeling in a two-photon interferometer," *Phys. Rev. A*, vol. 73, p. 063827, Jun 2006.
10. G. Grynberg, A. Aspect, and C. Fabre, *Introduction to Quantum Optics*. CUP, 2010.
11. R. Glauber, *Quantum theory of optical coherence*. WILEY-VCH Verlag, 2007.
12. A. Peres, *Quantum theory: Concepts and Methods*, vol. 72 of *Fundamental Theories of Physics*. Kluwer Academic, 2002.
13. L. Mandel, "Photon interference and correlation effects produced by independent quantum sources," *Phys. Rev. A*, vol. 28, p. 929–943, Aug 1983.
14. A. A. Clerk, M. H. Devoret, S. M. Girvin, F. Marquardt, and R. J. Schoelkopf, "Introduction to quantum noise, measurement, and amplification," *Rev. Mod. Phys.*, vol. 82, p. 1155–1208, Apr 2010.
15. P. Busch, "On the energy-time uncertainty relation. Part I: Dynamical time and time indeterminacy," *Foundations of Physics*, vol. 20, no. 1, p. 1–32, 1990.
16. T. Miyadera, "Energy-Time Uncertainty Relations in Quantum Measurements," *Foundations of Physics*, vol. 46, no. 11, p. 1522–1550, 2016.
17. Y. Aharonov and D. Bohm, "Time in the Quantum Theory and the Uncertainty Relation for Time and Energy," *Phys. Rev.*, vol. 122, p. 1649–1658, Jun 1961.
18. J. C. Diels and W. Rudolph, *Ultrashort Laser Pulse Phenomena: Fundamentals, Techniques, and Applications on a Femtosecond Time Scale, Academic Press, 2nd edition, Elsevier 2006*. Elsevier Science Publishers, 2nd edition ed., 2006.
19. Z. Ficek and S. Swain, *Quantum interference and coherence: theory and experiments*. Springer New York, 2005.

20. Y. Aharonov, D. Z. Albert, and L. Vaidman, "How the result of a measurement of a component of the spin of a spin- 1/2 particle can turn out to be 100," *Phys. Rev. Lett.*, vol. 60, p. 1351–1354, Apr 1988.
21. S. Kocsis, B. Braverman, S. Ravets, M. J. Stevens, R. P. Mirin, L. K. Shalm, and A. M. Steinberg, "Observing the Average Trajectories of Single Photons in a Two-Slit Interferometer," *Science*, vol. 332, no. 6034, p. 1170–1173, 2011.
22. N. Garcia, I. G. Saveliev, and M. Sharonov, "Time-Resolved Diffraction and Interference: Young's Interference with Photons of Different Energy as Revealed by Time Resolution," *Philosophical Transactions: Mathematical, Physical and Engineering Sciences*, vol. 360, p. 1039–1059, May 2002.
23. L. G. de Peralta, "Phenomenological quantum description of the ultrafast response of arrayed waveguide gratings," *Journal of Applied Physics*, vol. 108, no. 10, p. 103110, 2010.
24. W. C. Myrvold and J. Christian, *Quantum Reality, Relativistic Causality, and Closing the Epistemic Circle*. Springer Netherlands, 2009.
25. B.-G. Englert, "Fringe Visibility and Which-Way Information: An Inequality," *Phys. Rev. Lett.*, vol. 77, no. 11, p. 2154–2157, 1996.
26. R. Kaltenbaek, B. Blaumensteiner, M. Zukowski, M. Aspelmeyer, and A. Zeilinger, "Experimental Interference of independent photons," *Phys. Rev. Lett.*, vol. 96, p. 240502, 2006.
27. P. A. M. Dirac, *The principles of quantum mechanics*. OUP, 4th ed., 1978.
28. C. M. Caves, "Quantum mechanics of measurements distributed in time. A path-integral formulation," *Phys. Rev. D*, vol. 33, p. 1643–1665, Mar 1986.
29. R. P. Feynman, "Space-Time approach to non-relativistic quantum mechanics," *Rev. Mod. Phys.*, vol. 20, no. 2, 1948.
30. R. Feynman, A. Hibbs, and D. Styer, *Quantum Mechanics and Path Integrals*. Dover Books on Physics, Dover Publications, 2010.
31. C. Roychoudhuri, *Causal Physics: Photons by Non-Interactions of Waves*. CRC Press, Taylor and Francis, 2017.
32. H. Paul, "Interference between independent photons," *Rev. Mod. Phys.*, vol. 58, p. 209–231, Jan 1986.